Abdominal Radiology (2019) 44:1773–1784
https://doi.org/10.1007/s00261-018-01887-z

HEPATOBILIARY

The utility of diffusion-weighted imaging in improving the sensitivity of LI-RADS classification of small hepatic observations suspected of malignancy

Mohammad Abd Alkhalik Basha[1] · Rania Refaat[2] · Faten Fawzy Mohammad[1] · Mai E. M. Khamis[1] · Ahmed Mohamed El-Maghraby[1] · Ahmed A. El Sammak[1] · Rania M. Al-Molla[1] · Heba A. E. Mohamed[1] · Ahmad Abdullah Alnaggar[1] · Hanan Abdelhameed Hassan[1] · Taghreed M. Azmy[1] · Ahmed M. Alaa Eldin[1] · Mostafa Mohamad Assy[1] · Mohamad Zakarya AlAzzazy[1] · Khaled Mohamed Altaher[1] · Heba Fathy Tantawy[1] · Sameh Saber[1] · Mohamed I. Amin[1] · Ahmed Mohamed Alsowey[1] · Mohamed Hesham Saleh Radwan[1] · Heba F. Taha[3] · Talaat Fathy[4] · Amr Shaaban Hanafy[5] · Eman H. Abdelbary[6]

Published online: 2 January 2019

Abstract

Purpose We investigated the added value of diffusion-weighted imaging (DWI)/apparent diffusion coefficient (ADC) in the categorization of small hepatic observation (≤20 mm) detected in patients with chronic liver disease in reference to LI-RADS (liver imaging reporting and data system) classification system.

Methods We prospectively evaluated 165 patients with chronic liver disease with small hepatic observations (≤20 mm) which were previously categorized as LI-RADS grade 3–5 on dynamic contrast-enhanced CT (DCE-CT). All patients were submitted to a functional MRI including DCE and DWI. Using LI-RADS v2017, two radiologists independently evaluated the observations and assigned a LI-RADS category to each observation using DCE-MRI alone and combined DCE-MRI and DWI/ADC. In the combined technique, the radiologists assigned a LI-RADS category based on a modified LI-RADS criteria in which restricted diffusion on DWI was considered a major feature of HCC. We evaluated the inter-reader agreement with Kappa statistics and compared the diagnostic performance of the LI-RADS with two imaging techniques by Fisher's exact test using histopathology as the reference standard.

Results Combined technique in LI-RADS yielded better sensitivities (reader 1, 97% [65/67]; reader 2, 95.5% [64/67]) for HCC diagnosis than DCE-MRI alone (reader 1, 80.6% [54/67], $p=0.005$; reader 2, 83.6% [56/67], $p=0.04$). The specificities were insignificantly lower in combined technique (reader 1, 88.4% [107/121]; reader 2, 77.7% [94/121]) than in DCE-MRI alone (reader 1, 90.9% [110/121], $p=0.67$; reader 2, 79.3% [96/121], $p=0.88$). The inter-reader agreement of the LI-RADS scores between combined technique and DCE-MRI was good ($\kappa=0.765$).

Conclusion The use of DWI/ADC as an additional major criterion, improved the sensitivity of LI-RADS in the diagnosis of HCC while keeping high specificity.

Keywords LI-RADS · Perfusion MRI · DWI · Hepatocellular Carcinoma

✉ Mohammad Abd Alkhalik Basha
drmohammad_basha@yahoo.com

[1] Department of Radiodiagnosis, Zagazig University, Zagazig, Egypt

[2] Department of Radiodiagnosis, Ain Shams University, Cairo, Egypt

[3] Department of Medical Oncology, Zagazig University, Zagazig, Egypt

[4] Department of Tropical Medicine, Zagazig University, Zagazig, Egypt

[5] Department of Internal MEDICINE, Hepatology Division, Zagazig University, Zagazig, Egypt

[6] Department of Pathology, Zagazig University, Zagazig, Egypt

Introduction

Recent years have seen enormous advances in the multimodality management of hepatocellular carcinoma (HCC), which have produced considerable improvement in prognosis of HCC patients. Consequently, early detection of liver observations, accurate diagnosis of HCC, and tumor staging for treatment planning have become increasingly important. [1–3]. The Liver Imaging Reporting and Data System (LI-RADS) was introduced by the American College of Radiology (ACR) for the first time in 2011 and most recently updated in 2017 at the time of initiation of this study. LI-RADS was designed to standardize radiologic diagnosis of HCC [4–6]. Five major criteria are used to assign LI-RADS category: observation size, arterial phase hyperenhancement, washout appearance, capsule appearance, and threshold growth [4]. There are multiple ancillary features that give preferentiality to malignancy and can be used to upgrade LI-RADS category, including diffusion-weighted images (DWI) [4, 7, 8].

DWI is an MRI technique that is based on the restriction of water molecule motion. DWI provides both qualitative and quantitative information as an adjunct to conventional sequences. Apparent diffusion coefficient (ADC) measurements with DWI obtained at two or more *b* values allow quantitative analysis of diffusion [9, 10]. In tumorous tissues, it is thought to detect the restriction of the motion of water molecules that is associated with the decrease in the extracellular space caused by high cellularity [11]. DWI may be able to provide additional information for the detection of tumors or the differentiation of HCC from dysplastic nodules [12, 13].

Several studies have investigated the value of DWI in the diagnosis of HCC in patients with chronic liver disease, but few such studies have used LI-RADS [14, 15]. Accordingly, we conducted this prospective study to determine the diagnostic performance and added value of LI-RADS with combined dynamic contrast-enhanced MRI (DCE-MRI) and DWI/ADC technique in categorization of small hepatic observations (≤ 20 mm) suspected of malignancy using histopathology as the reference standard. Also, we aimed to reveal if an additional major criterion of DWI improves the diagnostic performance of LI-RADS for HCC in patients with chronic liver disease.

Patients and methods

Ethical considerations

The present study was approved by the institutional review board. All patients were informed about the study and provided written informed consent. The study was performed in accordance with the ethical principles of the Declaration of Helsinki.

Study population

This prospective study was conducted from January 2017 to May 2018. One hundred eighty-four adult consecutive patients were enrolled in the study.

Inclusion criteria

1. Patients with chronic liver disease.
2. Patients with CT-detected hepatic observations ≤ 20 mm in size and categorized as LR3–5.
3. Untreated observations.

All patients were submitted to a functional MRI including, DCE and DWI and histopathology after surgery or biopsy.

Liver DCE-MRI technique

All MRI examinations were conducted within 2 weeks of the CT examinations. All examinations were performed on a 1.5-Tesla MR system (Achieva-class IIa, Philips Medical Systems) using a phased-array torso coil. The patients held their breath in and expiration. All patients underwent transverse T1-weighted and T2-weighted MRI and multiphasic contrast-enhanced dynamic 3-dimensional MRI of the whole liver. The imaging technique included the following sequences: coronal true fast imaging with steady-state precession (True FISP) (field of view [FOV] = 35–40; repetition time/echo time [TR/TE] = 3/1.5 ms; matrix = 224 × 190; flip angle [FA] = 80°; section thickness [ST] = 5 mm; spacing = 2 mm), axial and coronal T1-weighted gradient echo in-phase and out-of-phase (FOV = 35–40; TR/TE = 117/4.6–2.3 ms; matrix = 224 × 190; FA = 80°; ST = 5 mm; spacing = 2 mm), axial heavily T2-weighted turbo spin echo (TSE) (FOV = 35–40; TR/TE = 416/120 ms; matrix = 224 × 190; FA = 90°; ST = 5 mm), and axial T1-weighted high-resolution isotropic volume examination (THRIVE) (FOV = 35–40; TR/TE = 3.9/1.85 ms; matrix = 224 × 190; FA = 10°; ST = 5 mm; spacing = 2 mm) before intravenous contrast injection and at arterial, portal

venous, and delayed phases after the injection of 0.1 mmol/kg gadolinium-diethylenetriamine pentaacetic acid (GdDTPA, Magnevist, Schering) administered at a rate of 2.0 mL/s followed by a 20-mL saline flush at a similar rate using a power injector (Medrad, Pittsburgh, Pennsylvania, USA) through a 20-gauge angiocatheter placed in the antecubital vein. The arterial, portal venous, and delayed phases were obtained at 30, 60, and 180 s from the start of contrast injection, respectively.

DWI/ADC technique

DWI and ADC maps were obtained before the administration of contrast by using a respiratory-triggered single-shot echo-planar imaging sequence with b values of 600 and 1000 mm^2/s applied in the z-direction: DWI with b value 600 (TR/TE, 1000/65, FA 90°, matrix: 128 × 128, section thickness 5–7 mm, intersection gap 1 mm and FOV 385 × 385 mm); DWI with b value 1000 (TR/TE, 1000/80, FA 90°, matrix: 128 × 128, section thickness 5–7 mm, intersection gap 1 mm and FOV 385 × 385 mm). The total acquisition time was 4 min 45 s. Quantitative ADC maps were derived automatically using commercially available software and an imaging workstation. On ADC maps, ADC values of the observation were measured by placing regions of interest (ROIs) centrally on the observation and occupying at least 50% of observation. The ADC values were measured twice, and the measurements were averaged. In case where there were multiple observations, the ADC value of the largest observation was measured.

Image analysis

All DCE-MRI and DWI/ADC data were transferred to the workstations and image analysis was performed on a dedicated platform Extended Brilliance Workstation (Philips Medical System, Best, The Netherlands) or PACS system (PaxeraUltima- paxeramed). The DCE-MRI and DWI/ADC images were separated for interpretation (i.e., the DCE-MRI image findings were reviewed without knowledge of the DWI/ADC findings). Two radiologists (reader 1 and 2) independently reviewed the DCE-MRI images. After 1 month, the same two radiologists (reader 1 and 2) independently reviewed the DCE-MRI and DWI/ADC images to diminish the memory bias of readers. The readers had more than 10 years of experience in hepatic MRI and were blinded to any clinical information or the results of the biopsy. The readers were asked to assign a LI-RADS category to all detected hepatic observations on DCE-MRI using the LI-RADS version 2017 algorithm. In the combined technique, the readers assigned a LI-RADS category based on a modified LI-RADS criteria in which restricted diffusion was considered a major feature of HCC and lack of restricted diffusion led to decreasing the category. Restricted diffusion was considered as hyperintensity signal on DWI at b values of 600 and 1000 mm^2/s and iso- or hypointensity signal on ADC map relative to adjacent liver parenchyma. Finally, each liver observation had 4 independent LI-RADS categories (two by DCE-MRI, and two by combined DCE-MRI and DWI).

Reference standard

The final diagnosis of the observations was confirmed based on histopathological findings after surgery ($n = 13$ patients) or percutaneous imaging-guided core biopsies [US guided ($n = 130$) or CT-guided ($n = 22$)]. In patients with multiple observations, the biopsy was obtained from the largest one and the biopsy result was considered the same for all observations. The biopsy was a part of the study and all biopsies were obtained within one or 2 weeks after MRI examination. All specimens were checked by two experienced pathologists and the results were obtained by consensus.

Statistical analysis

All statistical analyses were conducted using MedCalc (version 11.1; MedCalc, Mariakerke, Belgium). The Fleiss kappa (κ) statistics and 95% confidence intervals (CIs) were used to assess the inter-reader agreement (IRA) of imaging features and LI-RADS scoring results for the diagnosis of HCC. The κ values were interpreted as follows: poor agreement = 0.01–0.20; fair agreement = 0.21–0.40; moderate agreement = 0.41–0.60; good agreement = 0.61–0.80; and excellent agreement = 0.81–1.0. The diagnostic performance of LI-RADS with DCE-MRI and LI-RADS with combined technique was estimated per lesion. We used Fisher's exact test to assess statistically different sensitivities and specificities between two imaging datasets for each reader. Receiver operating characteristic (ROC) curve analysis was used to determine the cut-off value of ADC, the area under the curve (AUC), and the 95% CI. A p value ≤ 0.05 was considered statistically significant.

Results

Study population

Initially, we included 184 patients with chronic liver disease in our study. Nineteen patients were excluded from the study; three due to severe motion artifacts that rendered part of the dynamic phases or DWI of non-diagnostic quality and 16 due to indeterminate pathology results. This yielded a final cohort of 165 patients (127 males and 38 females, with an age range of 42–70 years and a mean age

Table 1 Patients' data

Characteristic	Value
No. of patients	165
No. of nodules	188
Age (years) mean ± SD (range)	55.6 ± 9.6 (42–70)
Sex of patients	
Male	127 (77)
Female	38 (23)
Cause of liver disease	
Hepatitis C	98 (59.4)
Hepatitis B	29 (17.6)
Hepatitis C and B	31 (18.8)
Primary biliary cirrhosis	4 (2.4)
Cirrhosis of unknown cause	3 (1.8)
Final diagnosis of nodules	
HCC	67 (35.6)
Non-HCC	121 (64.4)

Unless otherwise indicated, the data are represented number of observations with the corresponding percentages given in parentheses

SD standard deviation, *HCC* hepatocellular carcinoma

of 55.6 ± 9.6 years). The patients' data are summarized in Table 1. Every included patient had small hepatic observations (≤ 20 mm) and previously categorized as LI-RADS category 3–5 on DCE-CT examination. All patients were submitted to DCE-MRI with DWI/ADC technique. We detected a total of 188 observations. The final diagnoses in 188 observations were 67 HCCs and 121 non-HCCs (48 regenerative nodules and 73 dysplastic nodules).

DCE-MRI and DWI/ADC findings

Most of the non-HCCs showed low signal intensity (SI) on T2WI (reader 1, 86.8% [105/121]; reader 2, 83.5% [101/121]), but most HCCs showed high SI on T2WI (reader 1, 77.6% [52/67]; reader 2, 71.6% [48/67]). The difference of the SI distribution on T2WI was statistically significant between the two groups of observations ($p < 0.0001$ for both readers).

The SI patterns and ADC values of HCCs and non-HCCs on DWI and ADC map are presented in Table 2. Most of the non-HCCs showed low SI (reader 1, 91.7%; reader 2, 87.6%), but most HCCs showed high SI (reader 1, 95.5%; reader 2, 88.1%). The difference of the SI distribution was statistically significant between the two groups of observations ($p < 0.0001$ for both readers). The mean ADC values of the non-HCC were higher than that of the HCCs, and the difference between the two groups was statistically significant ($p = 0.0034$ and 0.0027 for reader 1 and 2, respectively).

Assignment of LI-RADS categories

We have summarized the determined LI-RADS categories of the hepatic observations depending on readers in Table 3. The change in individual patient observation on account of modified LI-RADS version, compared to DCE-MRI, according to reader 1 and reader 2 is presented in Tables 4 and 5, respectively.

In comparison to DCE-MRI, combined technique (reader 1 and 2) produces 7.4% [14/188 (HCC, 11; non-HCC, 3)] and 5.3% [10/188 (HCC, 8; non-HCC, 2)] upgrading of the observations, respectively, and 1.6% [3/188 (HCC, 0; non-HCC, 3)] and 2.1% [4/188 (HCC, 1; non-HCC, 3)] downgrading of the observations, respectively. Eight and six of LR4 observations are upgraded to LR5 by combined technique according to reader 1 and 2, respectively. All upgraded LR4 observations were HCCs. The combined technique reduces the number of LR3 and LR4 observations (reader 1, 4; reader 2, 3) and (reader 1, 102; reader 2, 90), respectively, compared to DCE-MRI (reader 1, 13; reader 2, 11), and (reader 1, 110; reader 2, 96), respectively.

Table 2 DWI/ADC findings

Lesion (No)		DWI signal intensity		ADC map		ADC value x 10^{-3} mm^2\sec Mean ± SD (range)	
		Reader 1	Reader 2	Reader 1	Reader 2	Reader 1	Reader 2
HCC (67)	High	64 (95.5)	59 (88.1)	2 (3)	5 (7.5)	1.19 ± 0.15 (1.06–1.4)	1.13 ± 0.23 (0.9–1.5)
	Low	2 (3)	6 (8.9)	61 (91)	54 (80.6)		
	Iso	1 (1.5)	2 (3)	4 (6)	8 (11.9)		
Non-HCC (121)	High	4 (3.3)	2 (1.7)	108 (89.3)	99 (81.8)	1.42 ± 0.26 (1.1–2)	1.44 ± 0.18 (1.2–1.8)
	Low	111 (91.7)	106 (87.6)	7 (5.7)	6 (5)		
	Iso	6 (5)	13 (10.7)	6 (5)	16 (13.2)		

Unless otherwise indicated, the data are represented number of observations with the corresponding percentages given in parentheses

HCC hepatocellular carcinoma, *DWI* diffusion-weighted imaging, *ADC* apparent diffusion coefficient, *SD* standard deviation

Table 3 LI-RADS categories of the 188 hepatic observations at DCE-MRI and modified LI-RADS version (combined DCE-MR and DWI/ADC) in relation to final diagnosis

LI-RADS Categories	DCE-MRI						Modified LI-RADS version (DCE-MR + DWI/ADC)					
	Reader 1			Reader 2			Reader 1			Reader 2		
	HCC	Non-HCC	Total	HCC	Non-HCC	Total	HCC	Non-HCC	Total	HCC	Non-HCC	Total
LR2	0	0	0	0	0	0	0	3	3	1	3	4
LR3	6	7	13	3	8	11	1	3	4	1	2	3
LR4	7	103	110	8	88	96	1	101	102	1	89	90
LR5	54	11	65	56	25	81	65	14	79	64	27	91
Total	67	121	188	67	121	188	67	121	188	67	121	188

The data are represented number of observations

HCC hepatocellular carcinoma, *DWI* diffusion-weighted imaging, *ADC* apparent diffusion coefficient

Table 4 Change in individual observation grading on account of modified LI-RADS version, compared to DCE-MRI, according to reader 1

DCE-MRI	Modified LI-RADS version (DCE-MR+DWI/ADC)				
	LR2	LR3	LR4	LR5	Total
LR2					0
LR3	3 (1.6)	4 (2.1)		6 (3.2)	13 (6.9)
LR4			102 (54.3)	8 (4.3)	110 (58.5)
LR5				65 (34.6)	65 (34.6)
Total	3 (1.6)	4 (2.1)	102 (54.3)	79 (42)	188

Table 5 Change in individual observation grading on account of modified LI-RADS version, compared to DCE-MRI, according to reader 2

DCE-MRI	Modified LI-RADS version (DCE-MR+DWI/ADC)				
	LR2	LR3	LR4	LR5	Total
LR2					0
LR3	4 (2.1)	3 (1.6)		4 (2.1)	11 (5.9)
LR4			90 (47.9)	6 (3.2)	96 (51.1)
LR5				81 (43.1)	81 (43.1)
Total	4 (2.1)	3 (1.6)	90 (47.9)	91 (48.4)	188

The data are represented as numbers with the corresponding percentages given in parentheses

The different colors indicate whether modified LI-RADS version upgraded (red), downgraded (green) or kept the stage the same (yellow) as DCE-MRI

LI-RADS Liver Imaging Reporting and Data System, *DWI* diffusion-weighted imaging, *ADC* apparent diffusion coefficient

Inter-reader agreement (IRA)

The IRA was excellent for the DWI and ADC signal intensity (κ = 0.857 and 0.838, respectively) and good for the ADC value, LI-RADS score, and major features (κ = 0.776, 0.765, and 0.656, respectively) (Table 6).

Table 6 Inter-reader agreement for imaging features of HCC and LI-RADS categorization within DCE-MRI and modified LI-RADS version (combined DCE-MR and DWI/ADC)

Feature	κ coefficients	95% CI
Major features	0.656	0.361–0.850
DWI signal intensity	0.858	0.791–0.925
ADC signal intensity	0.838	0.777–0.900
ADC value	0.776	0.651–0.900
LI-RADS	0.765	0.469–0.916

LI-RADS Liver Imaging Reporting and Data System, *HCC* hepatocellular carcinoma, *DCE-MRI* dynamic contrast-enhanced magnetic resonance imaging, *DWI* diffusion-weighted imaging, *ADC* apparent diffusion coefficient, *CI* Confidence interval

Diagnostic performance

The diagnostic performance of LI-RADS with DCE-MRI and combined DCE-MRI and DWI for HCC diagnosis is summarized in Table 7. Using the LI-RADS version 2017, our study demonstrated that LI-RADS with combined technique produced significantly higher sensitivities (reader 1, 97% [65/67]; reader 2, 95.5% [64/67]) for HCC diagnosis than using DCE-MRI alone (reader 1, 80.6% [54/67], $p = 0.005$; reader 2, 83.6% [56/67], $p = 0.04$). As regards specificity, there was no significant difference between combined technique (reader 1, 88.4% [107/121]; reader 2, 77.7% [94/121]) and DCE-MRI alone (reader 1, 90.9% [110/121], $p = 0.67$; reader 2, 79.3% [96/121], $p = 0.88$). Combined technique achieved significantly higher NPV (reader 1, 98.2% [107/109]; reader 2, 96.9% [94/97]) than DCE-MRI alone (reader 1, 89.4% [110/123], $p = 0.0007$; reader 2, 89.7% [96/107], $p = 0.05$). PPV were 69% to 83% for two imaging datasets, between which no statistical difference was observed ($p = 1.00$ and 0.87, respectively). The

Table 7 Diagnostic performance of LI-RADS with DCE-MRI and modified LI-RADS version (combined DCE-MRI and DWI) for confident HCC diagnosis

Criterion		Reader 1		Reader 2	
		%	95% CI	%	95% CI
DCE-MRI	Accuracy	87.2		80.9	
	Sensitivity	80.60	69.11–89.24	83.58	72.52–91.51
	Specificity	90.91	84.32–95.37	79.34	71.03–86.16
	PPV	83.08	71.73–91.24	69.14	57.89–78.93
	NPV	89.43	82.60–94.25	89.72	82.35–94.76
	AUC	0.86	0.80–0.90	0.81	0.75–0.87
Modified LI-RADS version (DCE-MR + DWI/ADC)	Accuracy	91.5		84	
	Sensitivity	97.01	89.63–99.64	95.52	87.47–99.07
	Specificity	88.43	81.35–93.53	77.69	69.22–84.75
	PPV	82.28	72.06–89.96	70.33	59.84–79.45
	NPV	98.17	93.53–99.78	96.91	91.23–99.36
	AUC	0.93	0.88–0.96	0.87	0.81–0.91

LI-RADS Liver Imaging Reporting and Data System, *HCC* hepatocellular carcinoma, *CT* computed tomography, *DCE-MRI* dynamic contrast-enhanced magnetic resonance imaging, *DWI* diffusion-weighted imaging, *ADC* apparent diffusion coefficient, *AUC* area under curve, *PPV* Positive Predictive Value, *NPV* Negative Predictive Value, *CI* Confidence interval

combined technique achieved higher AUC values (reader 1, 0.93 [0.88–0.96]; reader 2, 0.87 [0.81–91]) than DCE-MRI alone (reader 1, 0.86 [0.80–0.90]; reader 2, 0.81 [0.75–0.87]). However, the difference was not statistically significant ($p = 0.16$ and 0.32, respectively).

ROC analyses for ADC value

ROC analyses of the diagnostic performance of LI-RADS with ADC values for the definite diagnosis of HCC (reader 1, Fig. 1a) revealed an AUC of 0.811 (95% CI 0.520–965, $p = 0.01$), with the best threshold for confident HCC diagnosis of ≤ 1.1. The application of this threshold resulted in a sensitivity of 60% and a specificity of 88.9%. ROC analysis of the diagnostic performance of LI-RADS with ADC values for the definite diagnosis of HCC (reader 2, Fig. 1b) revealed an AUC of 0.867 (95% CI 0.583–0.985, $p < 0.008$), with the best threshold for confident HCC diagnosis of ≤ 1.16. The application of this threshold resulted in an 80% sensitivity and 100% specificity. Representative cases of our study are shown in Figs. 2, 3, and 4.

Discussion

Since its development, many attempts have been made to improve the LI-RADS classification system for a definite diagnosis of HCC. In this study, we wondered if an additional major criterion of DWI/ADC improves the diagnostic performance of LI-RADS for HCC in patients with chronic liver disease. Using the latest LI-RADS version and the modified LI-RADS criteria, our study demonstrated that if both DCE-MRI and DWI are combined as definitely indicating HCC, the specificities are minimally decreased, but the sensitivities are substantially increased (reader 1, 97%; reader 2, 95.5%). These findings are consistent with the results of previously published studies [12, 13, 16–18] which reported a sensitivity ranging from 77% to 97.87%. However, these studies did not use LI-RADS in diagnosis of HCC. Based on our findings, which resemble those of previously published studies, and in view of the significant diagnostic performance of DWI, we recommended the incorporation of DWI in LI-RADS classification system as a major criterion for the diagnosis of HCC, specifically for small observations suspected of malignancy.

Our study focused on patients who had a small (≤ 20 mm) observations as typically, the size of ≤ 20 mm is used as the size of cut-off for small observations in LI-RADS classification [4]. We also excluded larger (> 20 mm) observations as they are easily diagnosed.

Results on the additional value of T2WI in the diagnosis of HCC are discordant. In our study, we found that most HCCs showed high SI on T2WI and DWI, and low mean ADC value on ADC map. Hicks et al. [15] recommended the combination of T2 hyperintensity and restricted diffusion into a single ancillary feature in categorization of LR3–5 observations. Taouli and Koh [9] stated that absence of a corresponding decrease in ADC values compared to adjacent parenchyma suggests that the high SI on DWI is related to intrinsic T2 hyperintensity rather than to true diffusion restriction relative to adjacent parenchyma. Parikh et al. [19] reported that T2WI is poor for HCC detection, with

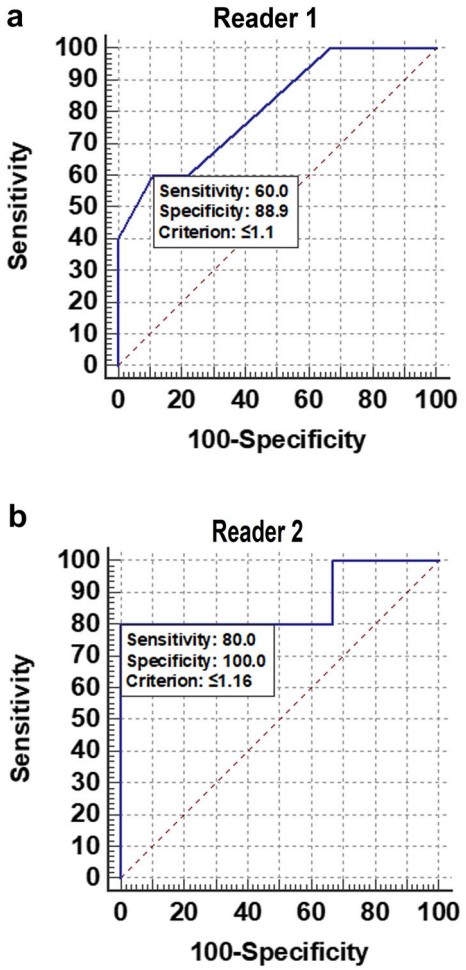

Fig. 1 Receiver operating characteristic (ROC) analyses of the diagnostic performance of LI-RADS with ADC values for the definite diagnosis of HCC as evidenced by pathology as a reference standard—reader 1 (**a**), and reader 2 (**b**). *HCC* hepatocellular carcinoma

improved detection by using DWI. Hecht et al. [20] found that the addition of T2WI modified the diagnosis in one out of 90 (1.1%) cases and barely increased diagnostic confidence; consequently, they recommend contrast-enhanced T1WI as a stand-alone sequence for the diagnosis of HCC. However, Kim et al. [21] showed that the addition of T2WI was helpful in the detection of HCC by increasing reader confidence. Nasu et al. [22] showed that there was a higher probability of HCCs being hyperintense on DWI than on T2WI (91.2% vs. 72.0%, respectively).

A consensus conference on DWI in cancer imaging stated that higher *b* values are needed in high vascular tissues [23, 24]. Ichikawa et al. [25] recommended using a *b* factor of > 400 s/mm^2 to achieve good and assessable DWI in abdominal MRI. Similarly, Vandecaveye et al. [12] compared *b* values of 0 s/mm^2, 100 s/mm^2, 600 s/mm^2, and 1000 s/mm^2, and stated that a *b* value of 600 s/mm^2 on DWI improved the detection of HCC, especially for tumors smaller than 2 cm. Most authors recommended *b* values in the range of 500 to 800 s/mm^2 for the evaluation of focal liver lesions [26, 27]. In the current study, we used two *b* values of 600 s/mm^2 and 1000 s/mm^2 on DWI. Using two *b* values in addition to two readers, help in calculating a precise ADC value with decreased regional ADC variations and decreased perfusion contamination.

In our study, 95.5% or 88.1% of HCCs displayed high signal intensity on DWI depending on the reader. This percentage is slightly higher than in previous studies. In the study by Piana et al. [16], 82% or 72% of HCCs were hyperintense depending on the reader. Nasu et al. [22] reported that around 91.2% of hypervascular HCCs were hyperintense.

The upgrading of some imaging features from ancillary to major may lead to grading variations potential, and it is necessary to explore how this upgrading actually takes effect on the imaging observation and the end-grading results of LI-RADS. Within this study, we made upgrading of DWI/ADC finding to become a major criterion. Our result revealed that in comparison to DCE-MRI, combined technique (reader 1 and 2) produced 7.4% and 5.3% upgrading of the observations, respectively, and 1.6% and 2.1% downgrading of the observations, respectively.

One of the potential advantages of combined technique is the reducing number of LR3 and LR4 observations. This increase in determination of LR3 and LR4 observations by combined technique has the potential to lead to decreased follow-up of observations that would not have been determined by DCE-MRI alone and decreased the need for biopsy.

Interestingly, in our study, some observations were categorized as LR3 based on DCE-MRI alone and upgraded to LR5 based on combined technique (6 observations by reader 1 and 4 observations by reader 2). This could be explained by the change in readers' perception of other major features when they considered the DWI in their scoring and not purely by counting restricted diffusion as a major feature, as readers simply got more sensitive to major features the second time around.

To the best of our knowledge, although few studies have compared the combined efficacy of DWI and DCE-MRI to that of DCE-MRI alone, this is the first prospective study in which we evaluated the diagnostic performance and inter-reader agreement of criteria combining the DWI and DCE-MRI in LI-RADS classification system for definite diagnosis of HCC. We found good to excellent agreement between the readers for the proposed criteria. The LI-RADS with combined technique had a good agreement (k = 0.765) with LI-RADS with DCE-MRI alone for detection of HCC. This result was similar to the result of Piana et al. [16] who reported that the inter-observer agreement for the DCE-MRI diagnostic criteria and their combination with DWI was good. Also, Shankar et al. [28] reported that DWI had a high

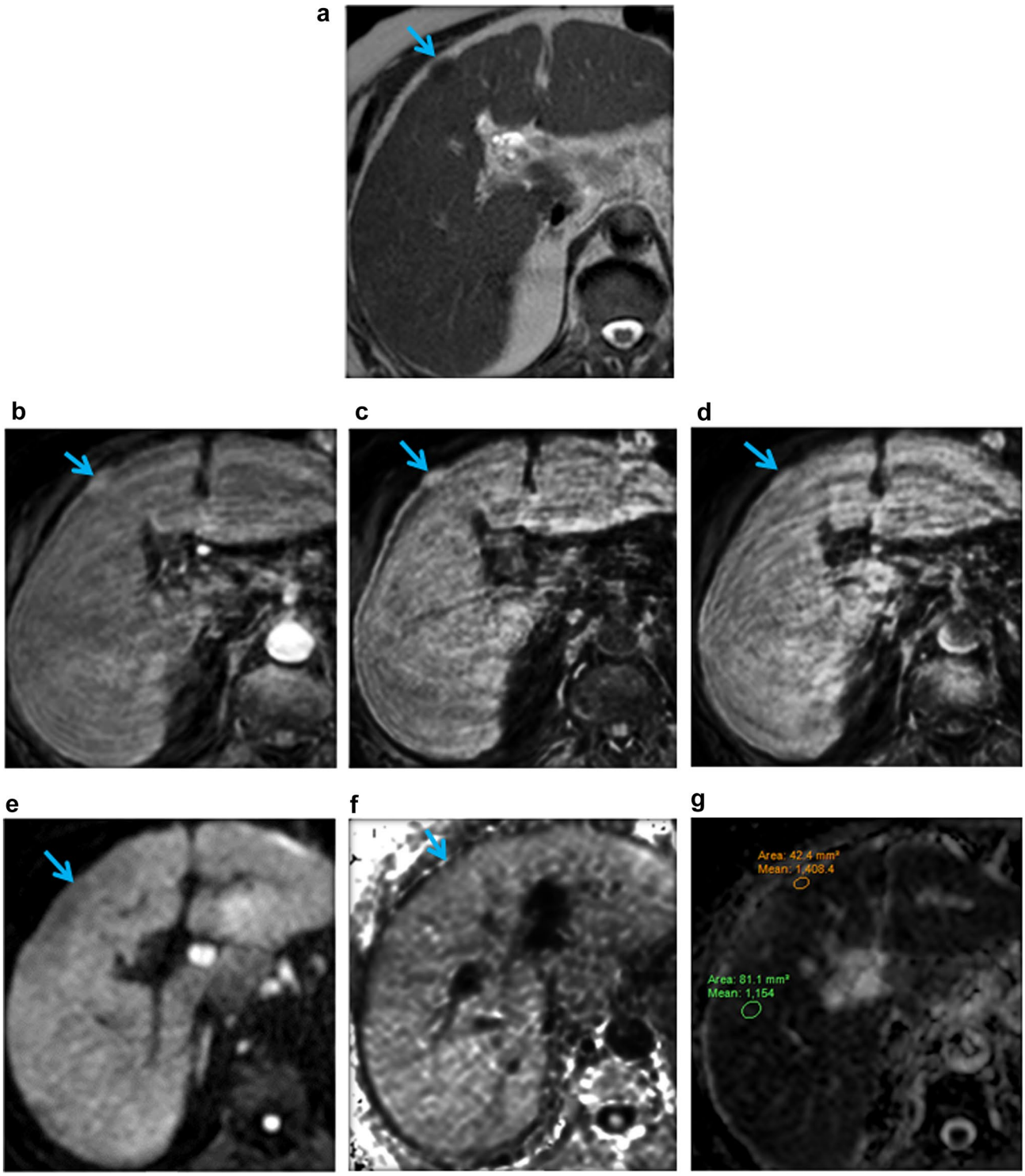

Fig. 2 A 42-year-old man with chronic liver disease due to hepatitis C virus presented by hepatic observation discovered on DCE-CT examination. **a** Axial T2WI shows subcapsular hypointense observation (15 mm) in segment V. **b** Axial T1WI postcontrast in arterial phase displays homogenous enhancement of the observation. **c**, **d** Axial T1WI postcontrast in portal and delayed phases show no washout of contrast. **e**, **f** Axial DWIs with b value 600 and b value 1000 demonstrate hypointensity of the observation. **g** Axial ADC map displays hyperintensity of the observation denoting unrestricted diffusion with ADC value equals 1.4×10^{-3}mm^2/sec. The observation was categorized as LR3 on DCE-MRI and LR2 on combined technique. Histopathology revealed regenerative nodule

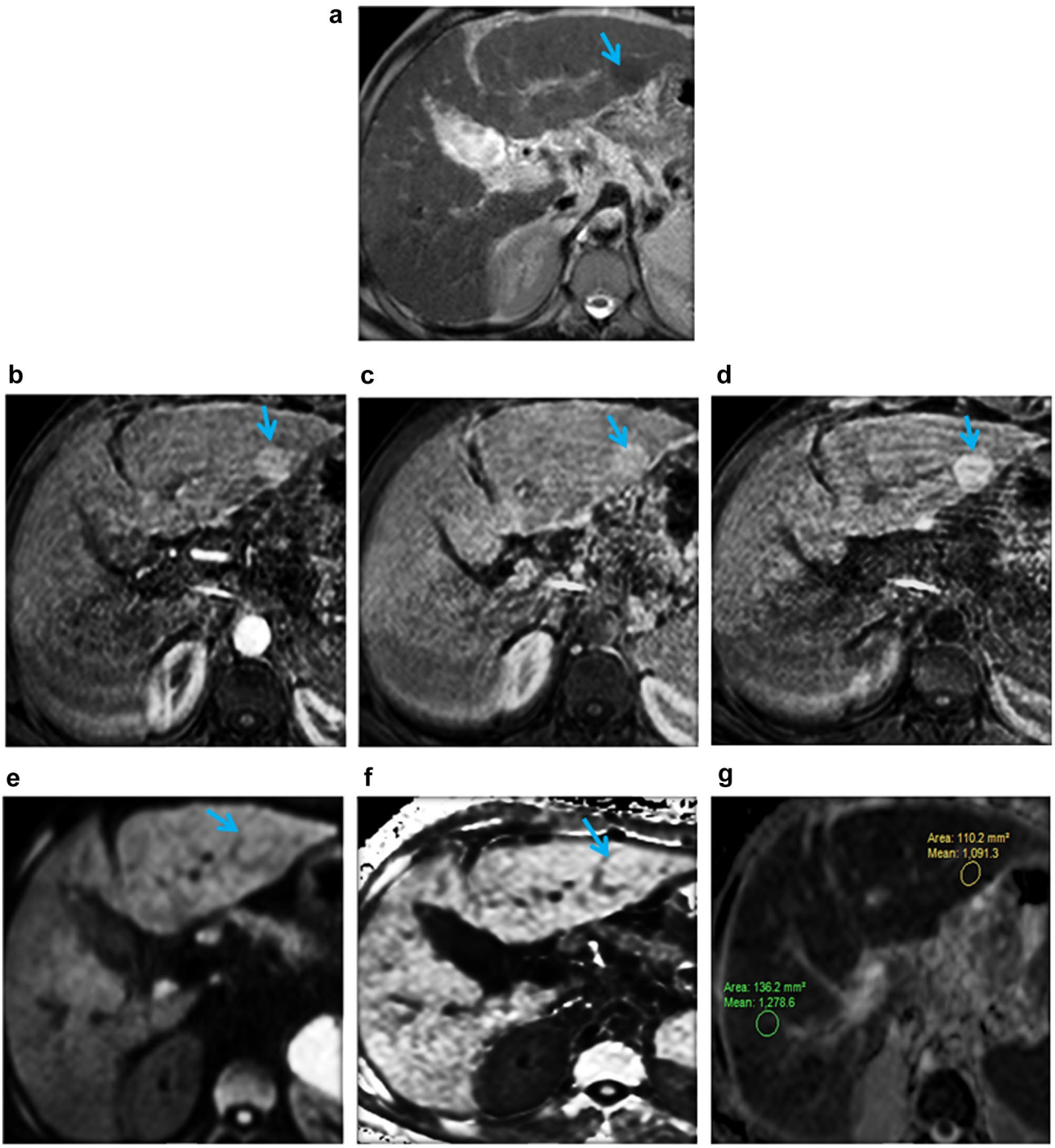

Fig. 3 A 43-year-old man with chronic liver disease due to hepatitis B virus presented by hepatic observation discovered on DCE-CT examination. **a** Axial T2WI shows subcapsular hypointense observation (20 mm) in segment II. **b** Axial T1WI postcontrast in arterial phase displays homogenous enhancement of the observation. **c**, **d** Axial T1WI postcontrast in portal and delayed phases show no washout of contrast. **e**, **f** Axial DWIs with b value 600 and b value 1000 demonstrate hyperintensity of the observation. **g** Axial ADC map displays hypointensity of the observation denoting restricted diffusion with ADC value equals $1.09 \times 10^{-3} mm^2/sec$. The observation was categorized as LR4 on DCE-MRI and LR5 on combined technique. Histopathology revealed high-grade dysplastic nodule

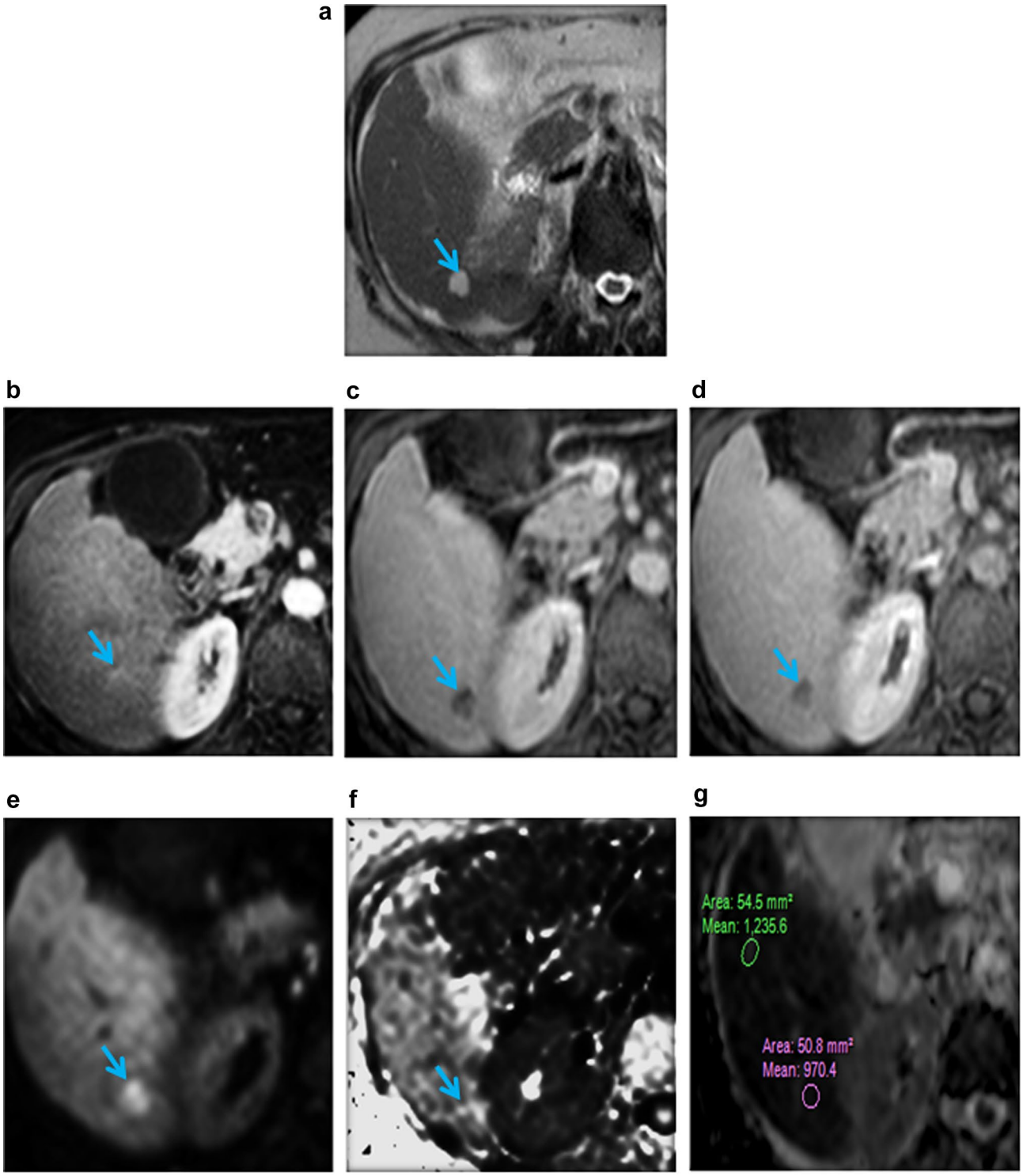

Fig. 4 A 55-year-old women with chronic liver disease due to hepatitis C virus presented by hepatic observations discovered on DCE-CT examination. **a** Axial T2WI shows hyperintense observation (13 mm) in segment VI. **b** Axial T1WI postcontrast in arterial phase displays partial enhancement of the observation. **c**, **d** Axial T1WI postcontrast in portal and delayed phases show washout of contrast. **e**, **f** Axial DWIs with b value 600 and b value 1000 demonstrate hyperintensity of the observation. **g** Axial ADC map displays hypointensity of the observation denoting restricted diffusion with ADC value equals 0.9×10^{-3}mm^2/s. The observation was categorized as LR4 on DCE-MRI and LR5 on combined technique. Histopathology revealed HCC

degree of agreement (k = 0.898) with DCE-MRI. According to the good agreement between the readers in our study, we encourage the inclusion of DWI as a major criterion in LI-RADS classification to improve the sensitivity for HCC.

We found that, although combined technique had a higher sensitivity for HCC than did DCE-MRI alone, relatively increased false-positive findings were seen with combined technique [reader 1, 7.4% (14/188); reader 2, 14.4% (27/188)] than with DCE-MRI [reader 1, 5.9% (11/188); reader 2, 13.3% (25/188)]. This relatively low specificity could be explained by five observations that showed imaging features suggestive by modified LI-RADs criteria as LR5 (arterial phase hyperenhancement with no washout, and high SI on DWI), and histopathology revealed high-grade dysplastic nodules.

The mean ADC values of HCCs reported in our study were nearly similar to that of other papers [29, 30]. Also, we found the best cut-off values of ≤ 1.1 or ≤ 1.16 depending on the readers were the same reported in the previous literature [31–33].

Finally, we consider that, according to our results, the LI-RADS with MRI may need advanced modifications to improve its diagnostic efficacy in patients with small hepatic observations suspected of malignancy. Our modified LI-RADS criteria based on upgrading diffusion restriction from ancillary to major imaging features demonstrated a significantly higher sensitivity and a non-significantly lower specificity than that of the classic LI-RADS criteria. This modified LI-RADS criteria allows evaluating all the observation which could arise in a cirrhotic liver, specifically the small observation (≤ 20 mm) suspected of malignancy such as early HCC, regenerative nodule and dysplastic nodule.

Our study has several strengths. It is a large, prospective study, which avoids the selection bias of retrospective study. However, our study has limitations. First, we concentrated our study on observations suspected of malignancy (LR3-5) and did not consider other benign LI-RADS categories (LR1 and LR2). Second, the absence of non-HCC malignancies (cholangiocarcinomas for example) in our study could represent a limitation in the estimation of the specificity. Third, we did not make subgroup analysis as regard tumor size or different b values. Fourth, some histological confirmations were obtained with liver biopsy, which in observations may lead to a small amount of sampling tissue and difficult observation characterization. However, we excluded the indeterminate pathology results from the study. Fifth, we had 23 observations without histopathological reference. Patients who have multiple hepatic observations are frequently encountered in the clinical practice. Therefore, we could not exclude them from our study. At the same time, it was extremely hard to get histologic confirmation of all obvious observations in the same patient owing to ethical and practical reasons. Subsequently, we followed such a scenario; obtained biopsy from the largest observation and considered the biopsy result was the same for all observations. Sixth, we only considered untreated observations. Finally, all MRI examinations were performed with an extracellular gadolinium contrast agent on a 1.5-Tesla MR system.

In conclusion, the addition of DWI/ADC as an additional major criterion increased the diagnostic sensitivity of LI-RADS for HCC while keeping high specificity, specifically for small observations suspected of malignancy. Future prospective studies with a large sample size should be performed to confirm or refute our results.

Acknowledgements The authors thank all staff members and colleagues in the Radiology Department-Zagazig University for their helpful cooperation and all the study participants for their patience and support.

Funding The authors state that this work has not received any funding.

Compliance with ethical standards

Conflict of interest The authors of this manuscript declare no relevant conflicts of interest, and no relationships with any companies, whose products or services may be related to the subject matter of the article.

Ethical approval Institutional review board approval was obtained.

Informed consent Written informed consent was obtained from all patients.

References

1. Bruix J, Sherman M (2011) Management of hepatocellular carcinoma: an update. Hepatology 53:1020–1022.
2. Kudo M, Matsui O, Izumi N, et al (2014) JSH consensus-based clinical practice guidelines for the management of hepatocellular carcinoma: 2014 update by the liver Cancer Study Group of Japan. Liver Cancer 3:458–468.
3. European Association For The Study Of The Liver (2012) EASL-EORTC clinical practice guidelines: management of hepatocellular carcinoma. J Hepatol 56: 908–943.
4. American College of Radiology (2014) Liver Imaging Reporting and Data System version 2014. Reston: American College of Radiology.
5. Cruite I, Tang A, Sirlin CB (2013) Imaging-based diagnostic systems for hepatocellular carcinoma. AJR 201:41–55.
6. Patella F, Pesapane F, Fumarola EM, et al (2018) CT-MRI LI-RADS v2017: A Comprehensive Guide for Beginners. Journal of Clinical and Translational Hepatology 6:1–5.
7. An C, Rakhmonova G, Choi JY, Kim MJ (2016) Liver imaging reporting and data system (LI-RADS) version 2014: understanding and application of the diagnostic algorithm. Clin Mol Hepatol 22:296–307.
8. Fusco R, Sansone M, Petrillo A (2015) The Use of the Levenberg-Marquardt and Variable Projection Curve-Fitting Algorithm in Intravoxel Incoherent Motion Method for DW-MRI Data Analysis. Appl Magn Reson 46:551–58.
9. Taouli B, Koh DM (2010) Diffusion-weighted MR imaging of the liver. Radiology 254:47–66

10. Galea N, Cantisani V, Taouli B (2013) Liver lesion detection and characterization: role of diffusionweighted imaging. J Magn Reson Imaging 37:1260–1276.
11. Koh DM, Collins DJ (2007) Diffusion-weighted MRI in the body: applications and challenges in oncology. AJR 188:1622–1635.
12. Vandecaveye V, De Keyzer F, Verslype C, et al (2009) Diffusion-weighted MRI provides additional value to conventional dynamic contrast enhanced MRI for detection of hepatocellular carcinoma. European Radiology 19:2456–66.
13. Xu PJ, Yan FH, Wang JH, et al (2010) Contribution of diffusion-weighted magnetic resonance imaging in the characterization of hepatocellular carcinomas and dysplastic nodules in cirrhotic liver. Journal of Computer Assisted Tomography 34:506–512.
14. Cha DI, Jang KM, Kim SH, Kang TW, Song KD (2017). Liver Imaging Reporting and Data System on CT and gadoxetic acid-enhanced MRI with diffusion-weighted imaging. European radiology 27:4394-4405.
15. Hicks RM, Yee J, Ohliger MA, et al (2016) Comparison of diffusion-weighted imaging and T2-weighted single shot fast spin-echo: Implications for LI-RADS characterization of hepatocellular carcinoma. Magnetic resonance imaging 34:915–921.
16. Piana G, Trinquart L, Meskine N, et al (2011) New MR imaging criteria with a diffusion-weighted sequence for the diagnosis of hepatocellular carcinoma in chronic liver diseases. J Hepatol 55:126–132.
17. Xu PJ, Yan FH, Wang JH, Lin J, Ji Y (2009) Added value of breath hold diffusion-weighted MRI in detection of small hepatocellular carcinoma lesions compared with dynamic contrast-enhanced MRI alone using receiver operating characteristic curve analysis. Journal of magnetic resonance imaging 29:341–349.
18. Wu LM, Xu JR, Lu Q, Hua J, Chen J, Hu J (2013) A pooled analysis of diffusion-weighted imaging in the diagnosis of hepatocellular carcinoma in chronic liver diseases. Journal of gastroenterology and hepatology 28:227–234.
19. Parikh T, Drew SJ, Lee VS, et al (2008) Focal liver lesion detection and characterization with diffusion-weighted MR imaging: comparison with standard breath-hold T2-weighted imaging. Radiology 246:812–822.
20. Hecht EM, Holland AE, Israel GM, et al (2006) Hepatocellular carcinoma in the cirrhotic liver: gadolinium-enhanced 3D T1-weighted MR imaging as a stand-alone sequence for diagnosis. Radiology 239:438–447.
21. Kim YK, Lee YH, Kim CS, Han YM (2008) Added diagnostic value of T2-weighted MR imaging to gadolinium-enhanced three-dimensional dynamic MR imaging for the detection of small hepatocellular carcinomas. Eur J Radiol 67:304–310.
22. Nasu K, Kuroki Y, Tsukamoto T, Nakajima H, Mori K, Minami M (2009) Diffusion-weighted imaging of surgically resected hepatocellular carcinoma: imaging characteristics and relationship among signal intensity, apparent diffusion coefficient, and histopathologic grade. AJR 193:438–444.
23. Muhi A, Ichikawa T, Motosugi U, et al (2009) High b-value diffusion weighted MR imaging of hepatocellular lesions: estimation of grade of malignancy of hepatocellular carcinoma. J Magn Reson Imaging 30:1005–1011.
24. Padhani AR, Liu G, Koh DM, et al (2009) Diffusion-weighted magnetic resonance imaging as a cancer biomarker: consensus and recommendations. Neoplasia 11:102–125.
25. Ichikawa T, Haradome H, Hachiya J, et al (1999) Diffusion-weighted MR imaging with single-shot echo-planar imaging in the upper abdomen: preliminary clinical experience in 61 patients. Abdom Imaging 24:456–461.
26. Kele PG, van der Jagt EJ (2010) Diffusion weighted imaging in the liver. World J Gastroenterol 16:1567–1576
27. Fowler KJ, Brown JJ, Narra VR (2011) Magnetic resonance imaging of focal liver lesions: approach to imaging diagnosis. Hepatology 54: 2227–2237
28. Shankar S, Kalra N, Bhatia A, et al (2016) Role of diffusion weighted imaging (DWI) for hepatocellular carcinoma (HCC) detection and its grading on 3T MRI: a prospective study. Journal of clinical and experimental hepatology 6:303–310.
29. Maiwald B, Lobsien D, Kahn T, Stumpp P (2014) Is 3-Tesla Gd-EOB-DTPA-enhanced MRI with diffusion-weighted imaging superior to 64-slice contrast-enhanced CT for the diagnosis of hepatocellular carcinoma? PloS one, 9 (11), e111935.
30. Inchingolo R, De Gaetano AM, Curione D, et al (2015) Role of diffusion-weighted imaging, apparent diffusion coefficient and correlation with hepatobiliary phase findings in the differentiation of hepatocellular carcinoma from dysplastic nodules in cirrhotic liver. European radiology 25:1087–1096.
31. Suh YJ, Kim MJ, Choi JY, et al (2012) Preoperative prediction of the microvascular invasion of hepatocellular carcinoma with diffusion-weighted imaging. Liver Transplantation 18:1171–1178.
32. Xu P, Zeng M, Liu K, et al (2014) Microvascular invasion in small hepatocellular carcinoma: is it predictable with preoperative diffusion-weighted imaging. Journal of Gastroenterology and Hepatology 29:330–336.
33. Okamura S, Sumie S, Tonan T, et al (2016) Diffusion-weighted magnetic resonance imaging predicts malignant potential in small hepatocellular carcinoma. Digestive and Liver Disease 48:945–952.